

Published in final edited form as:

*Cell Rep.* 2017 December 26; 21(13): 3708–3716. doi:10.1016/j.celrep.2017.12.006.

## Identification of Oxa1 Homologs Operating in the Eukaryotic Endoplasmic Reticulum

S. Andrei Anghel<sup>1,2</sup>, Philip T. McGilvray<sup>1</sup>, Ramanujan S. Hegde<sup>3</sup>, and Robert J. Keenan<sup>1,4,\*</sup>

<sup>1</sup>Department of Biochemistry and Molecular Biology, The University of Chicago, 929 East 57th Street, Chicago, IL 60637, USA

<sup>2</sup>Cell and Molecular Biology Graduate Program, The University of Chicago, 929 East 57th Street, Chicago, IL 60637, USA

<sup>3</sup>MRC Laboratory of Molecular Biology, Francis Crick Avenue, Cambridge CB2 0QH, UK

### Summary

Members of the evolutionarily conserved Oxa1/Alb3/YidC family mediate membrane protein biogenesis at the mitochondrial inner membrane, chloroplast thylakoid membrane, and bacterial plasma membrane, respectively. Despite their broad phylogenetic distribution, no Oxa1/Alb3/YidC homologs are known to operate in eukaryotic cells outside the endosymbiotic organelles. Here, we present bioinformatic evidence that the tail-anchored protein insertion factor WRB/Get1, the “endoplasmic reticulum (ER) membrane complex” subunit EMC3, and TMCO1 are ER-resident homologs of the Oxa1/Alb3/YidC family. Topology mapping and co-evolution-based modeling demonstrate that Get1, EMC3, and TMCO1 share a conserved Oxa1-like architecture.

Biochemical analysis of human TMCO1, the only homolog not previously linked to membrane protein biogenesis, shows that it associates with the Sec translocon and ribosomes. These findings suggest a specific biochemical function for TMCO1 and define a superfamily of proteins—the “Oxa1 superfamily”—whose shared function is to facilitate membrane protein biogenesis.

### Introduction

Membrane proteins must be inserted into the appropriate lipid bilayer to perform their biological functions and avoid toxic aggregation (Chiti and Dobson, 2006; Kopito, 2000). The existence of different types of membrane proteins and, in eukaryotes, different target membranes poses a challenge for the cellular biosynthetic machinery. To overcome this challenge, cells have evolved different pathways for insertion into membranes. The best understood of these is a co-translational pathway that delivers nascent polypeptides to the

---

This is an open access article under the CC BY-NC-ND license (<http://creativecommons.org/licenses/by-nc-nd/4.0/>).

\*Correspondence: bkeenan@uchicago.edu.

<sup>4</sup>Lead Contact

#### Author Contributions

R.S.H. and R.J.K. conceived of the project. S.A.A. and P.T.M. performed experiments. S.A.A. and R.J.K. wrote the manuscript with input from all authors.

#### Declaration of Interests

The authors declare no competing interests.

Sec translocon, a conserved proteinaceous channel in eukaryotes and prokaryotes. This pathway mediates insertion of most membrane proteins into the prokaryotic plasma membrane and the eukaryotic endoplasmic reticulum (ER) (Nyathi et al., 2013).

Some membrane proteins, however, are inserted independently of the translocon. For example, in eukaryotes, tail-anchored (TA) proteins are inserted into the ER membrane by the WRB-CAML complex (Get1-Get2 in yeast; Mariappan et al., 2011; Schuldiner et al., 2008; Vilardi et al., 2011; Wang et al., 2011, 2014; Yamamoto and Sakisaka, 2012). TA proteins are topologically simple, comprising a cytosolic-facing N-terminal domain and a single C-terminal transmembrane domain (TMD). The extreme C-terminal location of their TMD precludes targeting through the co-translational pathway. As a result, TA proteins utilize a Sec-independent post-translational pathway for insertion (Kutay et al., 1995; Stefanovic and Hegde, 2007). This pathway is conserved in eukaryotes, but whether it operates in bacteria and archaea remains unknown.

In bacteria, certain proteins are inserted into the plasma membrane by co- and post-translational, translocon-independent pathways mediated by YidC (Dalbey et al., 2014; Pross et al., 2016). These substrates are generally small, topologically simple proteins that lack large or highly charged translocated regions (Dalbey et al., 2014). YidC also functions in a translocon-dependent mode, where it facilitates the insertion, folding, and/or assembly of substrates containing multiple TMDs (Kuhn et al., 2017). Homologs of YidC are present in the mitochondrial inner membrane (called Oxa1 and Cox18) and the chloroplast thylakoid membrane (Alb3 and Alb4; Wang and Dalbey, 2011). Like bacterial YidC, these proteins function in different contexts as insertases, chaperones, and assembly factors.

Although YidC homologs are widely conserved among bacteria and archaea (Borowska et al., 2015), none have yet been identified in the eukaryotic endomembrane system. The absence of any such homolog has been puzzling, because the eukaryotic endomembrane system is derived from invagination of the plasma membrane of a prokaryotic ancestor (Cavalier-Smith, 2002). Here, we present evidence that the ER membrane possesses multiple proteins related to the Oxa1/Alb3/YidC family. These include the WRB/Get1 subunit of the TA protein insertase complex and two less understood but highly conserved proteins, TMCO1 and EMC3. We propose that these proteins are members of a superfamily—which we designate the “Oxa1 superfamily”—that all function broadly in membrane protein biogenesis.

## Results

### Phylogenetic and Functional Comparisons Define the Oxa1 Superfamily

In searching for archaeal homologs of the TA membrane protein insertion factor WRB/Get1, we identified a family of archaeal and eukaryotic membrane proteins annotated as “domain of unknown function 106” (DUF106) that are distantly related to the Oxa1/Alb3/YidC family (Figures 1A and 1B). The DUF106 group includes an archaeal family of uncharacterized membrane proteins, the eukaryotic “ER membrane complex” (EMC) subunit 3 (EMC3) family, and the eukaryotic “transmembrane and coiled coil domains 1” (TMCO1) family. DUF106 proteins appear to be phylogenetically ancient, as they are

present in the Asgard archaea, a group of organisms postulated to be the closest living relative of the last common ancestor of both archaeans and eukaryotes (Spang et al., 2015; Zaremba-Niedzwiedzka et al., 2017).

Consistent with these phylogenetic observations, there are clear functional similarities between members of the Oxa1/Alb3/YidC clade and members of the other clades for which some biochemical activity has been established (Figures 1C–1F). For example, during co-translational, translocon-independent insertion of a substrate protein into the bacterial plasma membrane, YidC binds to ribosome-nascent chain complexes (RNCs) and directly contacts the hydrophobic nascent chain (Kumazaki et al., 2014a, 2014b). Similarly, the archaeal DUF106 protein *Mj0480* (henceforth called the “YidC-like protein 1” or Ylp1) binds RNCs and can be crosslinked to a model substrate *in vitro* (Borowska et al., 2015). Moreover, the known translocon-independent substrates of YidC and Oxa1 and the post-translational substrates of Alb3 and WRB/Get1 are all simple membrane proteins with few transmembrane helices and small translocated regions (Aschtgen et al., 2012; Hegde and Keenan, 2011; Wang and Dalbey, 2011). Finally, although its precise function remains to be defined, the EMC has been linked to ERAD and biosynthesis of multi-pass membrane proteins (Richard et al., 2013; Satoh et al., 2015). Given these phylogenetic and functional similarities, we propose to assign these proteins as members of a superfamily, which we hereafter refer to as the Oxa1 superfamily.

### Oxa1 Superfamily Members Share Topological and Structural Features

A key prediction is that, owing to their common ancestry and conserved function, all members of the Oxa1 superfamily share a common architecture. As noted previously (Borowska et al., 2015), comparison of the crystal structures of bacterial YidC (Kumazaki et al., 2014a, 2014b) and archaeal Ylp1 (Borowska et al., 2015) reveals considerable structural overlap, including a three-TMD core, an N-in/C-out orientation, a cytosolic coiled coil between the first two TMDs, and a lipid-exposed hydrophilic groove, which has been shown to contact substrate proteins (Figure 2A).

Secondary structure and topology predictions for Get1, TMC01, and EMC3 suggest they share this architecture (Figures 2B and S1), but the topology of these proteins has not been conclusively established. Indeed, a recent study proposed that TMC01 has an N-in/C-in topology, with only two TMDs and a luminal-facing coiled coil (Wang et al., 2016); this topology is incompatible with placement of TMC01 into the Oxa1 superfamily.

To define the topology of Get1, TMC01, and EMC3, we designed 3×Flag-tagged constructs containing a consensus glycosylation sequence at the N or C terminus or within the predicted cytosolic coiled coil or luminal loop regions (Figures 2B and S2A). In all cases, we observed glycosylation of the N terminus and the loop between the second and third TMDs and no glycosylation of the C terminus or the coiled coil domain (Figure 2C). These data are consistent with the observation that the Get1 coiled coil binds to the cytosolic targeting machinery (Mariappan et al., 2011; Stefer et al., 2011; Wang et al., 2011) and with proteomic analyses showing that serine residues in the coiled coil and C-terminal regions of TMC01 are phosphorylated by cytosolic kinases (Déphoure et al., 2008; Olsen et al., 2010).

We also performed an unbiased, 3D structure prediction of TMCO1, Get1, and EMC3 using distance restraints derived from evolutionarily coupled residue pairs (Wang et al., 2017). Remarkably, the top-ranked models for human TMCO1 and yeast Get1 recapitulated the core structural features of bacterial YidC and archaeal Ylp1 proteins, including a luminal N terminus, cytosolic-facing coiled coil and C terminus, and a three-TMD core (Figures 2D, S2B, and S2D). The top-ranked EMC3 models also possessed a three-TMD core and a coiled coil motif between the first two TMDs but showed physically implausible orientations for the coiled coil and C terminus (Figure S2C); this may reflect the limited number of available sequence homologs, the relatively larger size of EMC3, and the absence of any membrane bilayer energy term. Nevertheless, these models suggest that members of the Oxa1 superfamily share a membrane topology and core architecture.

### TMCO1 Interacts with the Ribosome and the Sec61 Translocon

A second prediction of the Oxa1 superfamily model is that all of the proteins function in some capacity in membrane protein biogenesis. To test this prediction, we focused on human TMCO1, the only member of the superfamily not yet linked to membrane protein biogenesis. TMCO1 is an ER-resident membrane protein that is conserved in most eukaryotes (Iwamuro et al., 1999). Genetic variations around *TMCO1* are linked to glaucoma (Burdon et al., 2011; Sharma et al., 2012), and nonsense mutations cause a disorder associated with craniofacial dysmorphisms, skeletal anomalies, and intellectual disability (Alanay et al., 2014; Caglayan et al., 2013; Xin et al., 2010).

We asked whether any of the interactions of TMCO1 are similar to those of the better characterized members of the Oxa1 superfamily. In the case of bacterial YidC, primary interaction partners include the Sec translocon and the ribosome (Figures 1C and 1D). We first explored whether TMCO1 is part of a complex with translating ribosomes, as would be expected if it functions in co-translational insertion like some members of the Oxa1 superfamily (Figures 1C and 1D).

When digitonin-solubilized HEK293 membranes were fractionated on a sucrose gradient, TMCO1 and Sec61 were present in the 80S ribosome fraction (Figure 3A). In contrast, Derlin-1, an abundant ER membrane protein not known to bind the ribosome, did not co-migrate with ribosomes. Next, we tested whether TMCO1 and Sec61 are part of the same ribosome-bound complex. After immunoprecipitating digitonin-solubilized membranes prepared from a 3×Flag-tagged TMCO1 HEK293 cell line (Figure S3A), we observed a complex containing TMCO1, Sec61, and ribosomes (Figure 3B). Thus, TMCO1-Sec61-ribosome complexes can be isolated from cells under native conditions.

We next explored whether TMCO1 can exist in complex with Sec61 in the absence of ribosomes, as is true for YidC (Botte et al., 2016; Duong and Wickner, 1997). To identify ribosome-independent complexes, we used antibodies that bind TMCO1 and Sec61 $\beta$  on epitopes expected to be occluded by a bound ribosome. After immunoprecipitating digitonin-solubilized canine pancreatic microsomes (which contain high levels of Sec61), the anti-TMCO1 antibody pulled down components of the Sec61 translocon (Figure 3C). As expected, none of the antibodies pulled down ribosomes or the control protein, Derlin-1.

This suggests that TMCO1 and Sec61 can exist in the same complex in the absence of ribosomes.

Finally, we asked whether TMCO1 has an intrinsic affinity for ribosomes, as is the case for Oxa1 and some YidC homologs with long, positively charged C-terminal regions (Jia et al., 2003; Seitz et al., 2014). To test this prediction, we incubated recombinant, purified TMCO1 (Figure S3B) with unprogrammed ribosomes isolated from rabbit reticulocyte lysate. After sedimentation through a sucrose cushion, we observed ribosome-dependent pelleting of TMCO1 (Figure 3D). This interaction was salt sensitive, could be stabilized by chemical crosslinking, and was specific, because high concentrations of bulk RNA did not disrupt the interaction (Figures 3D, S3C, and S3D). Thus, in addition to its conserved structural features, TMCO1 shares key functional properties with members of the Oxa1/Alb3/YidC family, consistent with the predictions of the Oxa1 superfamily hypothesis.

## Discussion

Our phylogenetic, topological, and functional data identify an unexpected evolutionary relationship among a diverse group of integral membrane proteins that together define the Oxa1 superfamily. These proteins include bacterial YidC and its homologs in mitochondria and chloroplasts, archaeal Ylp1 proteins, and three ER-resident proteins: WRB/Get1; EMC3; and TMCO1. The best characterized members of the superfamily function in membrane protein biogenesis (Figures 1C–1F). In particular, Oxa1/Alb3/YidC proteins facilitate the insertion, folding, and/or assembly of a variety of membrane proteins (Wang and Dalbey, 2011), whereas the WRB/Get1 subunit of the GET pathway transmembrane complex mediates the insertion of TA membrane proteins into the ER (Hegde and Keenan, 2011). Similarly, the EMC3 subunit of the ER membrane complex has been proposed to play a role in membrane protein quality control (Richard et al., 2013) and biogenesis (Sato et al., 2015).

The function of TMCO1 has been less clear. Here, we show that TMCO1 possesses an Oxa1-like architecture and that TMCO1-Sec61-ribosome complexes can be isolated from HEK293 cells under native conditions. We also show that TMCO1 can be isolated in ribosome-free complexes with Sec61 and that TMCO1 has an intrinsic affinity for ribosomes. These properties suggest that TMCO1 functions most analogously to bacterial YidC and may facilitate the co-translational insertion, folding, and/or assembly of newly synthesized membrane proteins into the ER membrane (Figures 1C and 1D).

This assignment is not incompatible with the previous proposal that TMCO1 functions as a  $\text{Ca}^{2+}$  channel (Wang et al., 2016). Indeed, other well-characterized membrane protein insertases, including the bacterial and eukaryotic Sec translocon (Sachelaru et al., 2017; Simon and Blobel, 1991; Simon et al., 1989; Wirth et al., 2003) and mitochondrial Oxa1 (Krüger et al., 2012), have also been shown to conduct ions. This activity is likely related to their ability to translocate polypeptides across a membrane bilayer, and the same may be true for TMCO1. Alternatively, TMCO1 may modulate the  $\text{Ca}^{2+}$  efflux properties of Sec61 (Erdmann et al., 2011; Lang et al., 2011) or facilitate the biogenesis of a protein that functions in  $\text{Ca}^{2+}$  transport.

We speculate that Oxa1 superfamily proteins are all descendants of an ancestral machine that could insert topologically “simple” membrane proteins into the bilayer. Over time, the need to handle more complex substrates with additional TMDs and/or larger translocated regions would have been satisfied by evolution of the translocon. Subsequently, Oxa1 superfamily members would have been freed to evolve more specialized functions in concert with other membrane-bound and soluble factors. This might manifest in the translocon-dependent chaperone activities of YidC and Alb3 and the evolution of eukaryotic WRB/Get1 and EMC3 to function in association with other integral membrane components. Likewise, adaptation of WRB/Get1 and Alb3 to post-translational insertion would have resulted from modification of their cytosolic-facing coiled coil and C terminus for binding to the TRC40/Get3- and cpSRP54-targeting factors, respectively, instead of the ribosome.

The Oxa1 superfamily illustrates how a single structural scaffold has been diversified to handle the insertion, folding, and assembly of different proteins into different cellular membranes. The shared characteristics of Oxa1/Alb3/YidC and WRB/Get1 translocon-independent substrates raises the possibility that Oxa1 superfamily members might, under certain circumstances, act on overlapping sets of substrates in the ER. Consistent with this idea, it is notable that disruption of WRB (Sojka et al., 2014; Vogl et al., 2016), TMC01 (Caglayan et al., 2013; Xin et al., 2010), or EMC3 (Ma et al., 2015) is non-lethal. Such functional redundancy would impart robustness to membrane protein biogenesis, particularly under conditions of stress (Aviram et al., 2016; Aviram and Schuldiner, 2014). Identifying the native substrates and molecular mechanisms underlying EMC3- and TMC01-mediated biogenesis are important topics for future investigation.

## Experimental Procedures

### Phylogenetic Analysis

The DUF106 protein from *M. jannaschii* (MJ0480/Y1p1) was identified by HHpred (Söding et al., 2005) as a remote archaeal homolog of eukaryotic WRB/Get1. Expanded searches of eukaryotic, bacterial, and archaeal proteomes subsequently revealed a set of remote homologs, including Oxa1/Alb3/YidC, WRB/Get1, EMC3, TMC01, and archaeal Y1p1 proteins (Figure 1).

For each of these protein families, homologs were retrieved using PSI-Blast (Altschul et al., 1997) with an expected threshold cutoff of  $10^{-1}$ . An effort was made to include organisms as phylogenetically diverse as possible. Proteins in this list were then aligned using MUSCLE (Edgar, 2004). Gaps in the alignment were trimmed using TrimAl (Capella-Gutiérrez et al., 2009) with a cutoff of 0.4. A maximum-likelihood phylogenetic tree was built using PhyML-SMS (Guindon and Gascuel, 2003) using nearest-neighbor interchange (NNI) and the Akaike information criterion.

### TMC01 and EMC3 Topology Analysis by Glycosylation Mapping

An N-terminally 3×Flag-tagged human TMC01 construct, codon-optimized for bacterial expression, was subcloned into the pGFP plasmid (Clontech). EMC3 plasmids were identical but contained a cDNA-derived EMC3 sequence. The resulting constructs encode a

3×Flag-tagged protein under the control of a cytomegalovirus (CMV) promoter and an SV40 polyA signal. An opsin N-glycosylation tag (MNGTEGPNFYVPFSNKTVD) was then inserted at the indicated positions (Figure S2A). Transfections were performed by mixing 10 µg of DNA with 20 µL of Trans-It 293 reagent (Mirus Bio) in serum-free DMEM medium, incubating for 20 min at room temperature, and then adding to one 10-cm cell culture dish of HEK293 TRex TCMO1 KO (for TCMO1 transfections) or HEK293 TRex cells (for EMC3 transfection) at ~90% confluency. Cells were subcultivated 1:2 the next day and harvested 48 hr after transfection.

The membrane fraction was prepared as described in the Supplemental Experimental Procedures. The membranes were resuspended in 100 µL of 1% SDS with 100 mM DTT, incubated for 5 min at 95°C, and then cooled at room temperature. Buffer was adjusted to 50 mM HEPES (pH 7.4), 150 mM NaCl, 1% NP40, and 0.1% SDS and supplemented with 50 units of Benzonase (Sigma; E1014) and then split in half and treated with or without 20 units of PNGase F (Promega). Reactions were incubated for 4 hr at 37°C and then trichloroacetic acid (TCA) precipitated, resuspended in Laemmli Sample Buffer, and analyzed by SDS-PAGE.

### Get1 Topology Analysis by Glycosylation Mapping

A C-terminally 3×Flag-tagged *S. cerevisiae* Get1 sequence was subcloned into Yeplac195 under the control of the endogenous promoter and a CYC1 terminator. The opsin N-glycosylation tag was inserted at the indicated positions (Figure S2A). Plasmids were transformed into BY4741 yeast using the lithium acetate method (Gietz and Woods, 2002).

For glycosylation mapping experiments, yeast cells were picked off selective plates and grown for 1 hr in SD –URA +2% glucose at room temperature with 225 rpm shaking. Four  $A_{600}$  units were then collected and mixed with sodium azide to a final concentration of 0.01%, placed on ice, and lysed through a modified alkaline lysis method (Kushnirov, 2000). Cells were collected by centrifuging 3 min at  $16,000 \times g$  and then resuspended in 350 mM freshly diluted NaOH supplemented with 1 mM PMSF and 1× cOmplete, Mini, EDTA-free Protease Inhibitor Cocktail tablets (Roche). After a 5-min incubation on ice, cells were collected by centrifuging 3 min at  $16,000 \times g$  and the supernatant was discarded. The cell pellet was resuspended in 120 µL of 1% SDS, 100 mM DTT, and 50 mM Tris (pH 6.8) and incubated for 5 min at 95°C, cooled to room temperature, and centrifuged 3 min at  $16,000 \times g$  to remove insoluble material. Only the supernatant was processed further. Buffer was adjusted to 5 mM Tris (pH 6.8), 50 mM HEPES (pH 7.4), 150 mM NaCl, 1% NP40, and 0.1% SDS and supplemented with 25 units of Benzonase (Sigma; E1014), split in half, and then treated with or without 20 units of PNGase F (Promega). Reactions were incubated for 4 hr at 37°C and then TCA precipitated, resuspended in Laemmli Sample Buffer, and analyzed by SDS-PAGE.

### TMD Prediction and 3D Modeling

Transmembrane domain predictions were made with PolyPhobius (Käll et al., 2005) and TOPCONS (Tsirigos et al., 2015); coiled coil predictions were made with COILS (Lupas et al., 1991). RaptorX-Contact (Wang et al., 2017) was used to calculate contact maps from

alignments of 584 TMCO1 (188 residues), 453 EMC3 (261 residues), 442 Get1 (235 residues), and 485 WRB (174 residues) sequences from different species. RaptorX-Contact uses sequence conservation, residue co-evolution, and contact occurrence patterns to improve contact prediction in difficult cases like these, where only relative few sequence homologs are available. Template-free 3D modeling was done in CNS (Brünger et al., 1998) using the predicted contacts as distance restraints, as implemented in the <http://raptorx.uchicago.edu/ContactMap/> web server.

The 3D models for yeast Get1 and EMC3 show distortions in the highly charged coiled coil (Get1 and EMC3) and C-terminal regions (EMC3). In particular, these regions are observed to bend backward into the bilayer rather than extending away from it (Figures S2B and S2C). These non-physiologic conformations likely reflect the inclusion of a spurious restraint(s) in the 3D modeling, which does not explicitly account for the membrane (Wang et al., 2017). Thus, we constructed a hybrid model of Get1, in which the distorted coiled coil was replaced with the crystallographically defined Get1 coiled coil (PDB 3ZS8) by manually docking it as a rigid body between TM1 and TM2 (Figure 2D). Notably, in a covariation-based 3D model of WRB (the human homolog of Get1), the coiled coil adopts an energetically reasonable conformation (Figure S2B). No attempt was made to model EMC3 further, because no structural information is available for this protein.

### Assay for *In Vivo* Association of TMCO1 with Ribosomes

The total HEK293 cell membrane fraction (in assay buffer: 150 mM potassium acetate; 50 mM HEPES [pH 7.4]; and 5 mM magnesium acetate) was solubilized by addition of recrystallized digitonin (Calbiochem; lot no. 2913883) from a 5% stock to a final concentration of 2%. Solubilization was allowed to proceed for 30 min at 4°C with end over end mixing and then insoluble material was removed by centrifugation for 10 min at 10,000 × *g*. The soluble material was then layered over a 1-mL sucrose cushion (150 mM KCl, 50 mM Tris [pH 7.4], 5 mM MgCl<sub>2</sub>, 1 M sucrose, and 0.1% digitonin). Sucrose cushions were pelleted for 2 hr at 250,000 × *g* in a TLA100.3 rotor (Belin et al., 2010). The pellet was resuspended in the same buffer, re-run over a cushion again, and then finally the resuspended pellet was pelleted through a gradient (10%–50% sucrose, 150 mM potassium acetate, 50 mM Tris [pH 7.5], 5 mM MgCl<sub>2</sub>, and 0.1% digitonin) at 130,000 × *g* (SW28.1; Beckman Coulter) for 12 hr at 4°C. 900 μL fractions were collected manually from the top of the gradient, TCA precipitated, and analyzed by SDS-PAGE.

### Co-immunoprecipitation Analyses

For co-immunoprecipitations from canine pancreatic membranes (Promega), the membranes were resuspended in a buffer containing 250 mM potassium acetate, 50 mM HEPES (pH 7.4), 5 mM magnesium acetate, 15% glycerol, and 3% recrystallized digitonin (Calbiochem; Kun et al., 1979). Solubilization was allowed to proceed for 30 min on ice, and then insoluble material was removed by centrifugation for 10 min at 10,000 × *g*. The soluble material was then divided equally and layered over protein A resin that had been crosslinked to antibodies against TMCO1, Sec61β, or 3F4 (as control). Immunoprecipitation (IP) reactions were incubated for 2 hr at 4°C with end-over-end mixing and then washed six times with 250 mM potassium acetate, 50 mM HEPES (pH 7.4), 5 mM magnesium acetate,



15% glycerol, and 0.1% digitonin. Bound proteins were eluted by three successive 10-min incubations with 1 M glycine (pH 3) supplemented with 0.1% Fos-choline-12. Elutions were then TCA precipitated, resuspended in Laemmli Sample Buffer, and analyzed by SDS-PAGE.

For co-immunoprecipitations from 3×Flag-TMCO1 HEK293 TRex cells, the membrane fraction was isolated and washed twice with 250 mM potassium acetate, 50 mM HEPES (pH 7.4), 10 mM magnesium acetate, and 250 mM sucrose. Membranes were then resuspended in buffer containing 250 mM sucrose, 300 mM potassium acetate, 50 mM HEPES (pH 7.4), and 10 mM magnesium acetate. Solubilization was allowed to proceed for 30 min on ice, and then insoluble material was removed by centrifugation for 10 min at 10,000 × *g*. The soluble fraction was then added to anti-Flag M2 resin (Sigma) and incubated for 1 hr at 4°C with end-over-end mixing and then washed four times with 350 mM potassium acetate, 50 mM HEPES (pH 7.4), 5 mM magnesium acetate, 250 mM sucrose, and 0.1% digitonin. Bound proteins were eluted by 2 successive 30-min incubations with same buffer as the wash but supplemented with 0.5 mg/mL 3×Flag peptide (ApexBio). The elutions were then layered over a 1-mL sucrose cushion (150 mM KCl, 50 mM Tris [pH 7.4], 5 mM MgCl<sub>2</sub>, 1 M sucrose, and 0.1% digitonin) and then pelleted for 2 hr at 250,000 × *g* at 4°C in a TLA100.3 rotor (Belin et al., 2010). The supernatant was discarded, and the ribosome pellet was resuspended in 2× Laemmli Sample Buffer for analysis.

## Supplemental Information

Refer to Web version on PubMed Central for supplementary material.

## Acknowledgments

We thank T. Starr for advice with the phylogenetic tree construction; B. Zalisko for digitonin recrystallization; R. Rock, D.A. Drummond, and F. Bezanilla for sharing equipment; D. Bishop for the yeast strain; and Keenan and Hegde lab members for advice. This work was supported by NIH R21 EY026719 (to R.J.K.) and the UK Medical Research Council MC\_UP\_A022\_1007 (to R.S.H.). S.A.A. was supported by a Boehringer Ingelheim Fonds Ph.D. fellowship, and P.T.M. was supported by NIH training grant T32 GM007183.

## References

- Alanay Y, Ergüner B, Utine E, Haçarız O, Kiper POS, Ta kran EZ, Perçin F, Uz E, Sa ıro lu M , Yuksel B, et al. TMCO1 deficiency causes autosomal recessive cerebrofaciothoracic dysplasia. *Am J Med Genet A*. 2014; 164:291–304.
- Altschul SF, Madden TL, Schäffer AA, Zhang J, Zhang Z, Miller W, Lipman DJ. Gapped BLAST and PSI-BLAST: a new generation of protein database search programs. *Nucleic Acids Res*. 1997; 25:3389–3402. [PubMed: 9254694]
- Aschtgen MS, Zoued A, Llobès R, Journet L, Cascales E. The C-tail anchored TssL subunit, an essential protein of the enteroaggregative *Escherichia coli* Sci-1 Type VI secretion system, is inserted by YidC. *MicrobiologyOpen*. 2012; 1:71–82. [PubMed: 22950014]
- Aviram N, Schuldiner M. Embracing the void—how much do we really know about targeting and translocation to the endoplasmic reticulum? *Curr Opin Cell Biol*. 2014; 29:8–17. [PubMed: 24662022]
- Aviram N, Ast T, Costa EA, Arakel EC, Chuartzman SG, Jan CH, Haßdenteufel S, Dudek J, Jung M, Schorr S, et al. The SND proteins constitute an alternative targeting route to the endoplasmic reticulum. *Nature*. 2016; 540:134–138. [PubMed: 27905431]

- Belin S, Hacot S, Daudignon L, Therizols G, Pourpe S, Mertani HC, Rosa-Calatrava M, Diaz JJ. Purification of ribosomes from human cell lines. *Curr Protoc Cell Biol.* 2010 Chapter 3, Unit 3.40.
- Borowska MT, Dominik PK, Anghel SA, Kossiakoff AA, Keenan RJ. A YidC-like protein in the archaeal plasma membrane. *Structure.* 2015; 23:1715–1724. [PubMed: 26256539]
- Botte M, Zaccari NR, Nijeholt JL, Martin R, Knoops K, Papai G, Zou J, Deniaud A, Karuppasamy M, Jiang Q, et al. A central cavity within the holo-translocon suggests a mechanism for membrane protein insertion. *Sci Rep.* 2016; 6:38399. [PubMed: 27924919]
- Brünger AT, Adams PD, Clore GM, DeLano WL, Gros P, Grosse-Kunstleve RW, Jiang JS, Kuszewski J, Nilges M, Pannu NS, et al. Crystallography & NMR system: a new software suite for macromolecular structure determination. *Acta Crystallogr D Biol Crystallogr.* 1998; 54:905–921. [PubMed: 9757107]
- Burdon KP, Macgregor S, Hewitt AW, Sharma S, Chidlow G, Mills RA, Danoy P, Casson R, Viswanathan AC, Liu JZ, et al. Genome-wide association study identifies susceptibility loci for open angle glaucoma at TMCO1 and CDKN2B-AS1. *Nat Genet.* 2011; 43:574–578. [PubMed: 21532571]
- Caglayan AO, Per H, Akgumus G, Gumus H, Baranoski J, Canpolat M, Calik M, Yikilmaz A, Bilguvar K, Kumandas S, Gunel M. Whole-exome sequencing identified a patient with TMCO1 defect syndrome and expands the phenotypic spectrum. *Clin Genet.* 2013; 84:394–395. [PubMed: 23320496]
- Capella-Gutiérrez S, Silla-Martínez JM, Gabaldón T. trimAl: a tool for automated alignment trimming in large-scale phylogenetic analyses. *Bioinformatics.* 2009; 25:1972–1973. [PubMed: 19505945]
- Cavalier-Smith T. The phagotrophic origin of eukaryotes and phylogenetic classification of Protozoa. *Int J Syst Evol Microbiol.* 2002; 52:297–354. [PubMed: 11931142]
- Chiti F, Dobson CM. Protein misfolding, functional amyloid, and human disease. *Annu Rev Biochem.* 2006; 75:333–366. [PubMed: 16756495]
- Dalbey RE, Kuhn A, Zhu L, Kiefer D. The membrane insertase YidC. *Biochim Biophys Acta.* 2014; 1843:1489–1496. [PubMed: 24418623]
- Dephoure N, Zhou C, Villén J, Beausoleil SA, Bakalarski CE, Elledge SJ, Gygi SP. A quantitative atlas of mitotic phosphorylation. *Proc Natl Acad Sci USA.* 2008; 105:10762–10767. [PubMed: 18669648]
- Duong F, Wickner W. Distinct catalytic roles of the SecYE, SecG and SecDFyajC subunits of preprotein translocase holoenzyme. *EMBO J.* 1997; 16:2756–2768. [PubMed: 9184221]
- Edgar RC. MUSCLE: multiple sequence alignment with high accuracy and high throughput. *Nucleic Acids Res.* 2004; 32:1792–1797. [PubMed: 15034147]
- Erdmann F, Schäuble N, Lang S, Jung M, Honigsmann A, Ahmad M, Dudek J, Benedix J, Harsman A, Kopp A, et al. Interaction of calmodulin with Sec61 $\alpha$  limits Ca<sup>2+</sup> leakage from the endoplasmic reticulum. *EMBO J.* 2011; 30:17–31. [PubMed: 21102557]
- Gietz RD, Woods RA. Transformation of yeast by lithium acetate/single-stranded carrier DNA/polyethylene glycol method. *Methods Enzymol.* 2002; 350:87–96. [PubMed: 12073338]
- Guindon S, Gascuel O. A simple, fast, and accurate algorithm to estimate large phylogenies by maximum likelihood. *Syst Biol.* 2003; 52:696–704. [PubMed: 14530136]
- Hegde RS, Keenan RJ. Tail-anchored membrane protein insertion into the endoplasmic reticulum. *Nat Rev Mol Cell Biol.* 2011; 12:787–798. [PubMed: 22086371]
- Iwamuro S, Saeki M, Kato S. Multi-ubiquitination of a nascent membrane protein produced in a rabbit reticulocyte lysate. *J Biochem.* 1999; 126:48–53. [PubMed: 10393320]
- Jia L, Dienhart M, Schramp M, McCauley M, Hell K, Stuart RA. Yeast Oxa1 interacts with mitochondrial ribosomes: the importance of the C-terminal region of Oxa1. *EMBO J.* 2003; 22:6438–6447. [PubMed: 14657017]
- Käll L, Krogh A, Sonnhammer EL. An HMM posterior decoder for sequence feature prediction that includes homology information. *Bioinformatics.* 2005; 21(Suppl 1):i251–i257. [PubMed: 15961464]
- Kopito RR. Aggresomes, inclusion bodies and protein aggregation. *Trends Cell Biol.* 2000; 10:524–530. [PubMed: 11121744]

- Krüger V, Deckers M, Hildenbeutel M, van der Laan M, Hellmers M, Dreker C, Preuss M, Herrmann JM, Rehling P, Wagner R, Meinecke M. The mitochondrial oxidase assembly protein1 (Oxa1) insertase forms a membrane pore in lipid bilayers. *J Biol Chem.* 2012; 287:33314–33326. [PubMed: 22829595]
- Kuhn A, Koch HG, Dalbey RE. Targeting and insertion of membrane proteins. *Ecosal Plus.* 2017; 7
- Kumazaki K, Chiba S, Takemoto M, Furukawa A, Nishiyama K, Sugano Y, Mori T, Dohmae N, Hirata K, Nakada-Nakura Y, et al. Structural basis of Sec-independent membrane protein insertion by YidC. *Nature.* 2014a; 509:516–520. [PubMed: 24739968]
- Kumazaki K, Kishimoto T, Furukawa A, Mori H, Tanaka Y, Dohmae N, Ishitani R, Tsukazaki T, Nureki O. Crystal structure of *Escherichia coli* YidC, a membrane protein chaperone and insertase. *Sci Rep.* 2014b; 4:7299. [PubMed: 25466392]
- Kun E, Kirsten E, Piper WN. Stabilization of mitochondrial functions with digitonin. *Methods Enzymol.* 1979; 55:115–118. [PubMed: 459838]
- Kushnirov VV. Rapid and reliable protein extraction from yeast. *Yeast.* 2000; 16:857–860. [PubMed: 10861908]
- Kutay U, Ahnert-Hilger G, Hartmann E, Wiedenmann B, Rapoport TA. Transport route for synaptobrevin via a novel pathway of insertion into the endoplasmic reticulum membrane. *EMBO J.* 1995; 14:217–223. [PubMed: 7835332]
- Lang S, Erdmann F, Jung M, Wagner R, Cavalie A, Zimmermann R. Sec61 complexes form ubiquitous ER Ca<sup>2+</sup> leak channels. *Channels (Austin).* 2011; 5:228–235. [PubMed: 21406962]
- Lupas A, Van Dyke M, Stock J. Predicting coiled coils from protein sequences. *Science.* 1991; 252:1162–1164. [PubMed: 2031185]
- Ma H, Dang Y, Wu Y, Jia G, Anaya E, Zhang J, Abraham S, Choi JG, Shi G, Qi L, et al. A CRISPR-based screen identifies genes essential for West-Nile-virus-induced cell death. *Cell Rep.* 2015; 12:673–683. [PubMed: 26190106]
- Mariappan M, Mateja A, Dobosz M, Bove E, Hegde RS, Keenan RJ. The mechanism of membrane-associated steps in tail-anchored protein insertion. *Nature.* 2011; 477:61–66. [PubMed: 21866104]
- Nyathi Y, Wilkinson BM, Pool MR. Co-translational targeting and translocation of proteins to the endoplasmic reticulum. *Biochim Biophys Acta.* 2013; 1833:2392–2402. [PubMed: 23481039]
- Olsen JV, Vermeulen M, Santamaria A, Kumar C, Miller ML, Jensen LJ, Gnad F, Cox J, Jensen TS, Nigg EA, et al. Quantitative phosphoproteomics reveals widespread full phosphorylation site occupancy during mitosis. *Sci Signal.* 2010; 3:ra3. [PubMed: 20068231]
- Pross E, Soussoula L, Seitz I, Lupo D, Kuhn A. Membrane targeting and insertion of the C-tail protein SciP. *J Mol Biol.* 2016; 428:4218–4227. [PubMed: 27600410]
- Richard M, Boulin T, Robert VJ, Richmond JE, Bessereau JL. Biosynthesis of ionotropic acetylcholine receptors requires the evolutionarily conserved ER membrane complex. *Proc Natl Acad Sci USA.* 2013; 110:E1055–E1063. [PubMed: 23431131]
- Sachelaru I, Winter L, Knyazev DG, Zimmermann M, Vogt A, Kuttner R, Ollinger N, Siligan C, Pohl P, Koch HG. YidC and SecYEG form a heterotetrameric protein translocation channel. *Sci Rep.* 2017; 7:101. [PubMed: 28273911]
- Satoh T, Ohba A, Liu Z, Inagaki T, Satoh AK. dPob/EMC is essential for biosynthesis of rhodopsin and other multi-pass membrane proteins in *Drosophila* photoreceptors. *eLife.* 2015; 4:e06306.
- Schuldiner M, Metz J, Schmid V, Denic V, Rakwalska M, Schmitt HD, Schwappach B, Weissman JS. The GET complex mediates insertion of tail-anchored proteins into the ER membrane. *Cell.* 2008; 134:634–645. [PubMed: 18724936]
- Seitz I, Wickles S, Beckmann R, Kuhn A, Kiefer D. The C-terminal regions of YidC from *Rhodospirillum rubrum* and *Oceanicaulis alexandrii* bind to ribosomes and partially substitute for SRP receptor function in *Escherichia coli*. *Mol Microbiol.* 2014; 91:408–421. [PubMed: 24261830]
- Sharma S, Burdon KP, Chidlow G, Klebe S, Crawford A, Dimasi DP, Dave A, Martin S, Javadiyan S, Wood JP, et al. Association of genetic variants in the TMCO1 gene with clinical parameters related to glaucoma and characterization of the protein in the eye. *Invest Ophthalmol Vis Sci.* 2012; 53:4917–4925. [PubMed: 22714896]

- Simon SM, Blobel G. A protein-conducting channel in the endoplasmic reticulum. *Cell*. 1991; 65:371–380. [PubMed: 1902142]
- Simon SM, Blobel G, Zimmerberg J. Large aqueous channels in membrane vesicles derived from the rough endoplasmic reticulum of canine pancreas or the plasma membrane of *Escherichia coli*. *Proc Natl Acad Sci USA*. 1989; 86:6176–6180. [PubMed: 2474828]
- Söding J, Biegert A, Lupas AN. The HHpred interactive server for protein homology detection and structure prediction. *Nucleic Acids Res*. 2005; 33:W244–W248. [PubMed: 15980461]
- Sojka S, Amin NM, Gibbs D, Christine KS, Charpentier MS, Conlon FL. Congenital heart disease protein 5 associates with CASZ1 to maintain myocardial tissue integrity. *Development*. 2014; 141:3040–3049. [PubMed: 24993940]
- Spang A, Saw JH, Jørgensen SL, Zaremba-Niedzwiedzka K, Martijn J, Lind AE, van Eijk R, Schleper C, Guy L, Ettema TJG. Complex archaea that bridge the gap between prokaryotes and eukaryotes. *Nature*. 2015; 521:173–179. [PubMed: 25945739]
- Stefanovic S, Hegde RS. Identification of a targeting factor for posttranslational membrane protein insertion into the ER. *Cell*. 2007; 128:1147–1159. [PubMed: 17382883]
- Stefer S, Reitz S, Wang F, Wild K, Pang YY, Schwarz D, Bomke J, Hein C, Löhr F, Bernhard F, et al. Structural basis for tail-anchored membrane protein biogenesis by the Get3-receptor complex. *Science*. 2011; 333:758–762. [PubMed: 21719644]
- Tsirigos KD, Peters C, Shu N, Käll L, Elofsson A. The TOPCONS web server for consensus prediction of membrane protein topology and signal peptides. *Nucleic Acids Res*. 2015; 43(W1):W401–W407. [PubMed: 25969446]
- Vilardi F, Lorenz H, Dobberstein B. WRB is the receptor for TRC40/Asn1-mediated insertion of tail-anchored proteins into the ER membrane. *J Cell Sci*. 2011; 124:1301–1307. [PubMed: 21444755]
- Vogl C, Panou I, Yamanbaeva G, Wichmann C, Mangosing SJ, Vilardi F, Indzhykulian AA, Pangršič T, Santarelli R, Rodriguez-Ballesteros M, et al. Tryptophan-rich basic protein (WRB) mediates insertion of the tail-anchored protein otoferlin and is required for hair cell exocytosis and hearing. *EMBO J*. 2016; 35:2536–2552. [PubMed: 27458190]
- Wang P, Dalbey RE. Inserting membrane proteins: the YidC/Oxa1/Alb3 machinery in bacteria, mitochondria, and chloroplasts. *Biochim Biophys Acta*. 2011; 1808:866–875. [PubMed: 20800571]
- Wang F, Whynot A, Tung M, Denic V. The mechanism of tail-anchored protein insertion into the ER membrane. *Mol Cell*. 2011; 43:738–750. [PubMed: 21835666]
- Wang F, Chan C, Weir NR, Denic V. The Get1/2 transmembrane complex is an endoplasmic-reticulum membrane protein insertase. *Nature*. 2014; 512:441–444. [PubMed: 25043001]
- Wang QC, Zheng Q, Tan H, Zhang B, Li X, Yang Y, Yu J, Liu Y, Chai H, Wang X, et al. TMCO1 is an ER Ca(2+) load-activated Ca(2+) channel. *Cell*. 2016; 165:1454–1466. [PubMed: 27212239]
- Wang S, Sun S, Li Z, Zhang R, Xu J. Accurate de novo prediction of protein contact map by ultra-deep learning model. *PLoS Comput Biol*. 2017; 13:e1005324. [PubMed: 28056090]
- Wirth A, Jung M, Bies C, Frien M, Tyedmers J, Zimmermann R, Wagner R. The Sec61p complex is a dynamic precursor activated channel. *Mol Cell*. 2003; 12:261–268. [PubMed: 12887911]
- Xin B, Puffenberger EG, Turben S, Tan H, Zhou A, Wang H. Homozygous frameshift mutation in TMCO1 causes a syndrome with craniofacial dysmorphism, skeletal anomalies, and mental retardation. *Proc Natl Acad Sci USA*. 2010; 107:258–263. [PubMed: 20018682]
- Yamamoto Y, Sakisaka T. Molecular machinery for insertion of tail-anchored membrane proteins into the endoplasmic reticulum membrane in mammalian cells. *Mol Cell*. 2012; 48:387–397. [PubMed: 23041287]
- Zaremba-Niedzwiedzka K, Caceres EF, Saw JH, Bäckström D, Juzokaite L, Vancaester E, Seitz KW, Anantharaman K, Starnawski P, Kjeldsen KU, et al. Asgard archaea illuminate the origin of eukaryotic cellular complexity. *Nature*. 2017; 541:353–358. [PubMed: 28077874]

### Highlights

- The “Oxa1 superfamily” comprises a group of membrane protein biogenesis factors
- Three ER-resident proteins, Get1, EMC3, and TMCO1, are members of the superfamily
- TMCO1, similar to bacterial YidC, associates with ribosomes and the Sec translocon

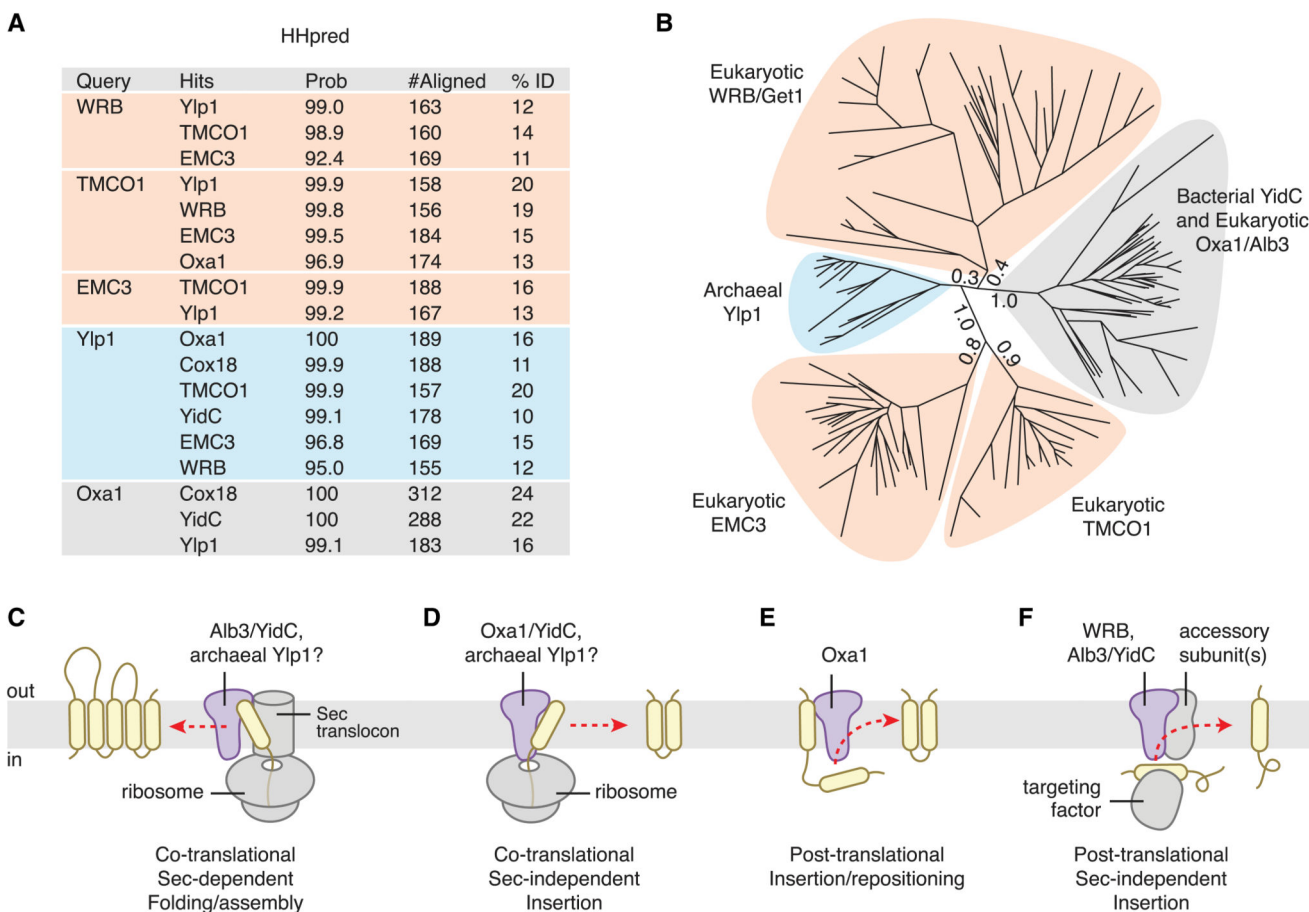


### Figure 1. Phylogenetic and Functional Comparison Defines the Oxa1 Superfamily

(A) Identification of remote DUF106 homologs using HHpred. Eukaryotic (human), bacterial (*E. coli*), and archaeal (*M. jannaschii*) proteomes were searched for each query (UniProt ID: WRB, O00258; Oxa1, Q15070; TMCO1, Q9UM00; EMC3, Q9P0I2; Ylp1, Q57904) using default settings in HHpred in “global” alignment mode. Top hits are listed, along with the HHpred probability score, the number of residues aligned, and the sequence identity.

(B) Maximum-likelihood tree of representative sequences. Branch lengths for the five main clades are indicated.

(C) During Sec-dependent, co-translational assembly and folding, substrates are delivered to the membrane by the ribosome; insertion requires participation of the Sec translocon. Substrates of this pathway typically contain multiple TMDs and/or large translocated regions. Superfamily members exemplifying this activity include bacterial YidC and chloroplast Alb3.

(D) During Sec-independent, co-translational insertion, topologically “simple” substrates that lack large or highly charged translocated regions are delivered to the membrane by the ribosome. Superfamily members exemplifying this activity include Oxa1 and YidC; archaeal Ylp1 proteins function similarly *in vitro*.

(E) Post-translational TMD repositioning, exemplified by Oxa1.

(F) During Sec-independent, post-translational insertion, topologically simple substrates are delivered to the membrane by soluble targeting factors. Superfamily members exemplifying this activity include WRB/Get1, which inserts tail-anchored proteins delivered by TRC40/Get3; chloroplast Alb3, which inserts specific proteins delivered to the thylakoid membrane by cpSRP43; and bacterial YidC.

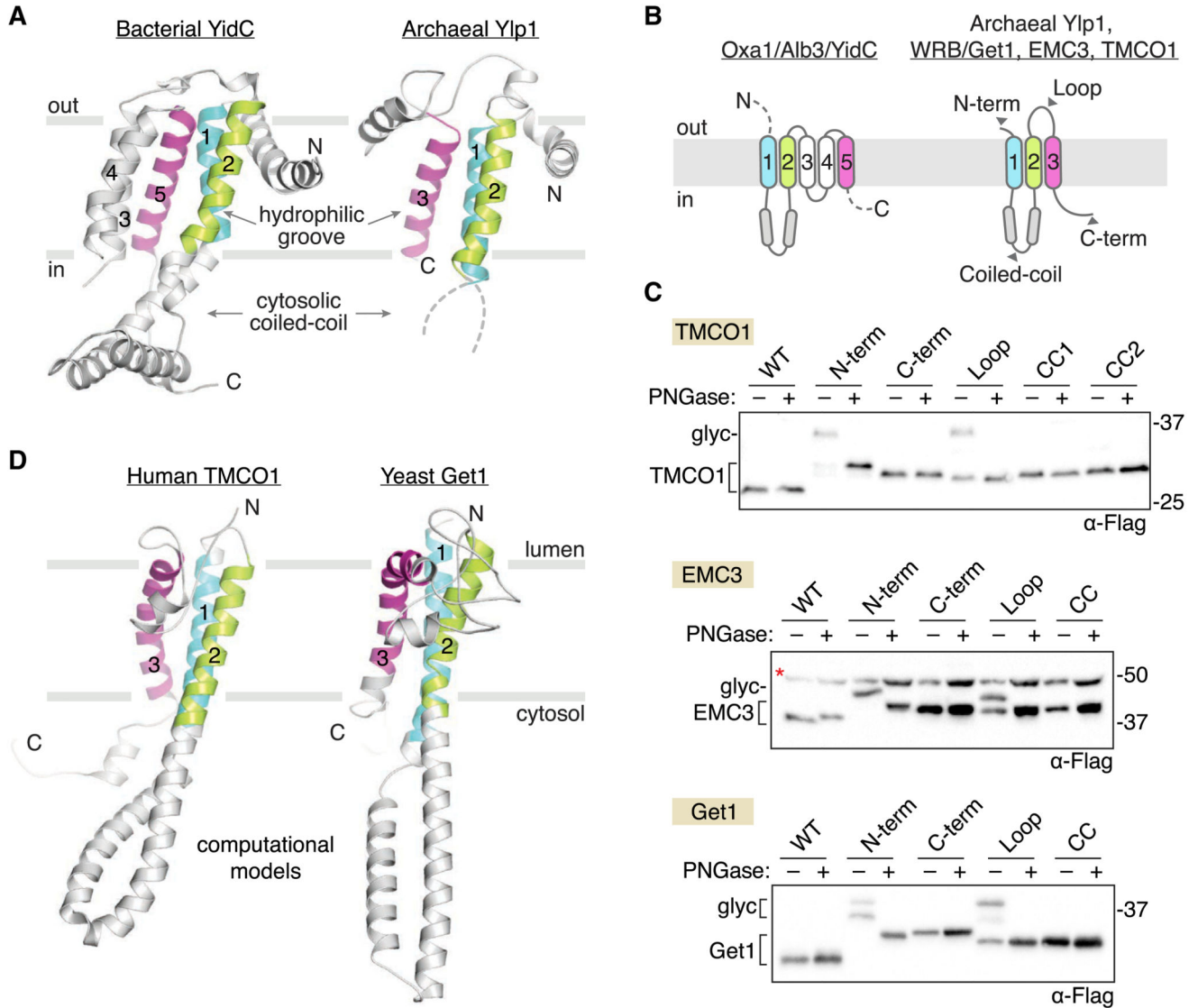


**Figure 2. Oxa1 Superfamily Members Share a Conserved Membrane Topology and Core Structural Features**

(A) Comparison of known structures from two clades: bacterial YidC (left; PDB 3WO6) and archaeal Ylp1 (right; PDB 5C8J). These proteins share a common N-out/C-in topology, a cytosolic-facing coiled coil between TM1 and TM2 (disordered in the archaeal structure), and a three-TMD core (colored) that harbors a lipid-exposed hydrophilic groove implicated in binding to nascent polypeptides during insertion.

(B) Predicted topology of the Oxa1 superfamily members.

(C) Experimentally defined topology of human TMCO1, EMC3, and yeast Get1.

Glycosylation acceptor sequences were introduced at the indicated positions (gray arrowheads in B and Figure S2), and glycosylation was monitored by western blotting after treatment with or without PNGase F. All three proteins conform to the predicted Oxa1 superfamily topology. A non-specific, cross-reacting band visible in all EMC3 samples is marked (red asterisk).



(D) Evolutionary covariation-based computational 3D models of human TMC01 and yeast Get1 recapitulate the core structural features of bacterial YidC and archaeal Ylp1: luminal N terminus; cytosolic-facing coiled coil and C terminus; and a three-TMD core. Here, the predicted coiled coil region of Get1 has been replaced with the experimentally determined structure of the Get1 coiled coil (PDB 3ZS8). The resulting hybrid model is in good agreement with the covariation-based 3D model calculated for human WRB (Figure S2). See also Figures S1 and S2.

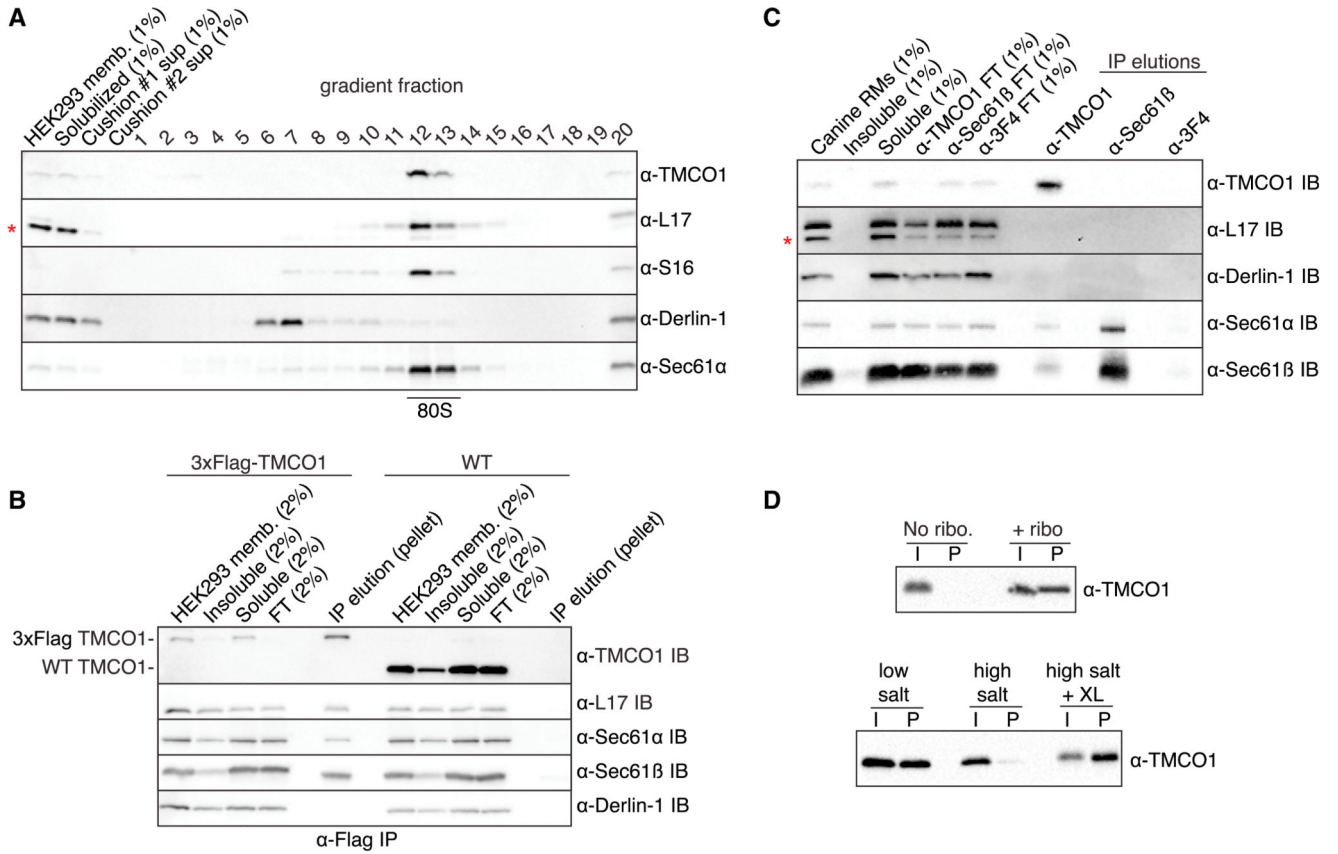


**Figure 3. TMCO1 Forms a Complex with the Sec61 Translocon and RNCs**

(A) HEK293 membranes were solubilized with digitonin, fractionated by sucrose cushion, separated on a high-resolution sucrose gradient, and analyzed by western blotting. TMCO1 co-fractionates with intact 80S particles and the Sec61 translocon, but not the unrelated ER membrane protein Derlin-1, which does not bind to ribosomes. Blots for the large (L17) and small (S16) ribosomal subunits are also shown; a non-specific, cross-reacting band visible in the L17 blot is indicated with an asterisk.

(B) Digitonin-solubilized membranes from wild-type (WT) HEK293 cells or a HEK293 cell line containing an N-terminal 3×Flag-tagged TMCO1 allele were analyzed by anti-Flag immunoprecipitation, sucrose cushion, and western blotting.

(C) Digitonin-solubilized canine pancreatic rough microsomes were tested for interaction between TMCO1 and Sec61 by co-immunoprecipitation and western blotting. An anti-TMCO1, but not a control anti-3F4 antibody, pulls down two components of Sec61. The absence of TMCO1 in the reciprocal pull-down is consistent with the higher levels of Sec61 in these membranes.

(D) Recombinant, purified TMCO1 co-sediments with unprogrammed ribosomes isolated from rabbit reticulocyte lysate (top panel). This interaction is salt sensitive and can be stabilized by chemical crosslinking (XL) (bottom panel). The pellet (P) fractions correspond to 5× volume equivalents of the input (I) fractions. See also Figure S3.